Mitigation of severe accidents for SFR and associated event sequence assessment

F. Bertrand, A. Bachrata, N. Marie, S. Kubo, Y. Onoda, A. Shibata, R. Kubota, B. Carluec

Version of Record: https://www.sciencedirect.com/science/article/pii/S0029549320304878
Manuscript_72d9d485e2c667addeb81cc546beb938

Mitigation of severe accidents for SFR and associated event sequence assessment

F. Bertrand[1*], A. Bachrata[1], N. Marie[1], S. Kubo[2] Y. Onoda[2], A. Shibata[3],R. Kubota[3], B. Carluec[4]

1 - CEA, DES, IRESNE, DER, F-13108, Saint Paul lez Durance, France
2 - JAEA, 4002 Narita, O-arai, Ibaraki 311-1393, Japan
3 - Mitsubishi FBR Systems, Inc.34-17, Jingumae 2-Chome, Shibuya-ku, Tokyo, 150-0001 Japan
4 – Framatome, 10 rue Juliette Récamier, 69006, France

Keywords

Severe accident studies, ASTRID, Mitigation strategy, DCS-M-TT efficiency, PIRT

Abstract

This article deals with the assessment of severe accident event sequence and mitigation strategy elaboration performed in the frame of ASTRID SFR Gen IV reactor project (le Coz et al., 2013), including the Japanese/French collaboration involving JAEA, MFBR, Framatome and CEA. In the first part of the paper, the mitigation strategy and the approach defined for the design of mitigation features, which are transverse tubes called DCS-M-TT are presented. By considering 21 DCS-M-TTs into the core as defined at the end of the conceptual design, which enable to extract the core materials and to significantly reduce the core reactivity within the order of 10 seconds in some typical accidental conditions, the accidental power excursions in ASTRID should not lead to a significant mechanical energy release, thus ensuring the integrity of the main vessel. Nevertheless, some loading assumptions independent from event evolutions have been defined in order to design the main vessel and the core catcher in order to cover extreme accident consequences and to get rid of event sequence dependency when designing the reactor. Then, SIMMER-IV (3D) the main calculation results of ULOF simulations whose goal was to verify the DCS-M-TT efficiency and to support a PIRT are highlighted in the paper. They confirmed that fuel discharge through discharge tubes has a large mitigating impact on power excursions. The last part of this paper deals with an approach dedicated to the description of severe accident event sequences through generic event trees (GETs), which logically summarize the representative courses of accident progression showing relationship between

*Corresponding author

critical causal events and major outcomes of the accidents. A set of trees has been elaborated for the description of each event sequence able to cause severe accidents (ULOF: unprotected loss of flow, UTOP: unprotected transient overpower and USAF: unprotected sub-assembly fault). The event-tree bifurcation points towards one branch or another of the possible event evolution could be examined alternatively with a help of phenomenological event chart (PECs). Afterwards, in association with the GET analysis, a PIRT (Phenomenon identification ranking table) on ULOF has been developed conjointly by Japanese and French sides in order to prioritize R&D needs. About 100 phenomena have been retained and classified depending on the various time periods of the accident event sequences; the primary phase, the short-term relocation phase, the expansion phase and the long-term relocation and cooling phase.

Glossary

ASTRID	advanced sodium technological reactor for industrial demonstration
CC	core catcher
CFV	low void worth core
CRGT	control rod guide tube
DCS-M-TT/TT	transfer tube dedicated to fuel discharge for mitigation
DHR	decay heat removal
DHRS	decay heat removal system
DHX	decay heat exchanger
EOEC	end of equilibrium cycle
FAIDUS	fuel assembly with inner duct structure
FCI	fuel coolant interaction
FoM	figure of merit
FRN	French team involved in this collaborating work
GET/ET	generic event tree/event tree
JPN	Japanese team involved in this collaborating work
JSFR	Japanese sodium fast reactor
PEC	phenomenological event chart
PFBR	prototype of fast breeder reactor
PIRT	phenomenological identification and ranking table
PNS	upper shielding
RV	reactor vessel
SA	sub-assembly

SA	severe accident
SASS	self-actuated shutdown system
SFR	sodium fast reactor
ULOF	unprotected loss of flow accident
USAF	unprotected sub-assembly fault
UTOP	unprotected transient overpower

1. Introduction

This paper consists in the synthesis of accidental event sequences assessment performed in the frame of the French/Japanese collaboration on ASTRID dedicated to severe accident (SA) reactor studies (Serre et al., 2017). When designing a SFR (Chellapandi et al., 2013, Kubo et al., 2015, Bertrand et al., 2018), severe accident prevention and mitigation is a crucial issue because SFR cores are not in their most reactive configuration (Waltar and Reynolds, 1981) as for instance LWR cores do. For this reason, when a SFR core is degraded and loses its geometry, some power excursions might happen for unprotected accident event sequences. In such a case, depending on the course of the accident, a large thermal energy might be released into the fuel and a part of it can be converted in mechanical energy (Masheck et al., 2018) that could threaten the main vessel leak tightness and integrity (Figure 1). In the frame of the ASTRID project, CEA and its partners have chosen to design a core (Table 1) with a safe natural behavior (Sciora et al., 2011), that is, not likely to lead to a significant mechanical energy release due to sodium vaporization, in particular thanks to a sodium plenum, an inner fertile zone and a so-called "diabolo" shape (Figure 1).

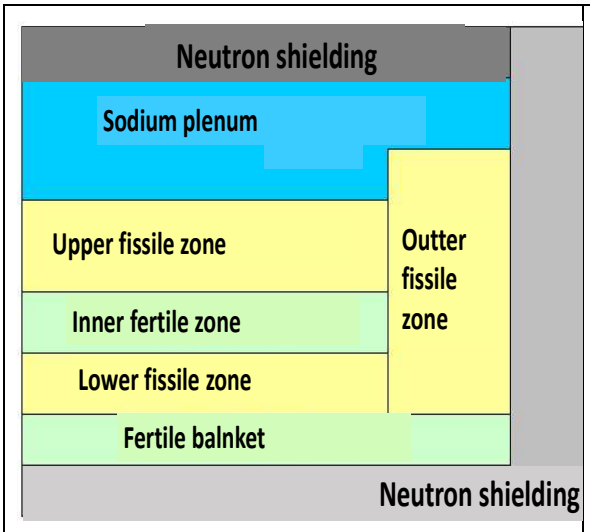

Vertical cut of the CFV core

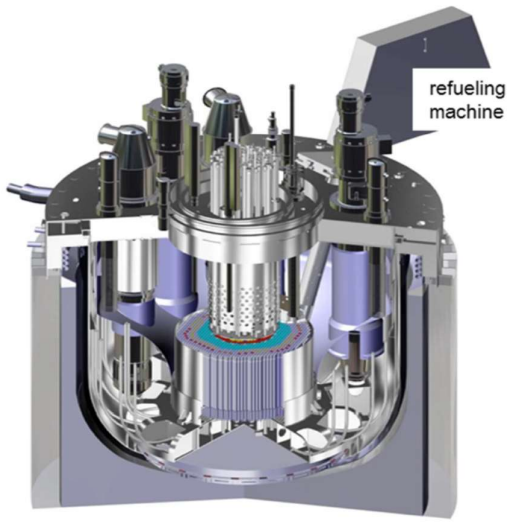

Astrid primary circuit arrangement

Figure 1: Sketches of ASTRID CFV core vertical cut and of primary vessel

Nominal thermal power [MW]	1,500
Inner fissile zone height (lower / upper) [cm]	25 / 35
Outer fissile zone height [cm]	90
Inner fertile zone height [cm]	20
Inner zone radius [cm]	133.5
Outer zone radius [cm]	162.6
Effective delayed neutron fraction (β_{eff}) [pcm]	368
Void reactivity effect ($), Core at equilibrium	- 0.5

Table 1: Main features of the CFV core

However, in order to be able to mitigate some very unfavorable cases and to retain core molten materials into the primary vessel, complementary safety devices have been added to the reactor design (Bertrand et al., 2018). The aim of this paper is to present the ASTRID severe accident mitigation strategy and the accident event sequence studies and the R&D supporting it. The severe accidents are initiated by sequences that could lead to core melting in case of an SFR reactor scram failure. These sequences are loss of primary flow (ULOF), transient overpower (UTOP) and sub-assembly faults (USAF). On the basis of event sequence evolutions, preliminary design and efficiency of mitigation devices verification (fuel discharge ducts, DCS-M-TT) are presented in this paper.

Section 2 is focused on mitigation device design process. Then, section 3 is devoted to studies performed in order to verify their efficiency. Some elements deal with the top-down and the so-called 'decoupled approach' retained in order to determine loading cases for the main vessel and for the core catcher. Finally, in section 4, the main insights of event sequence assessment with generic event trees (GET) are presented. They enable to define the phenomena and the configurations assessed by a PIRT. This PIRT dedicated to ULOF[2] is presented and several R&D topics worth to be investigated in priority are highlighted.

2. Mitigation strategy and mitigation device design process

In the section 2.1, devices implemented in other reactor or core projects are firstly recalled briefly. Then in the section 2.2, the mitigation objective and strategy for ASTRID are first recalled. Then, the design approach used for the main vessel is presented in section 2.3. Afterwards, the so-called "decoupled study approach" and the design features retained in order to achieve a preliminary design of mitigation tubes called DCS-M-TT, as well as the main parametric studies supporting their design, are presented in section 2.4. Finally, in section 2.5, assumptions retained for the loading cases supporting the core catcher design are briefly presented. These cases have been selected in order to show the relocated materials coolability and thus, as for light water reactor, to show the fuel in-vessel retention (Bachrata et al., 2012).

[2] PIRT activities has been started by ULOF since it gathers most of the phenomena involved in a core melting accident of a SFR.

2.1. Overview of the state of the art on fuel relocation dedicated device for mitigation

In former or in ongoing reactor designs, some mitigation devices were foresseen in order to limit the mechanical energy that could be released in case of power excursion. In the Japenese JSFR project (Kubo et al., 2015), despite the good core design and fuel characteristics aiming at eliminating the possibility of prompt criticality leading to mechanical loadings, so-called FAIDUS (Fuel Assembly with Inner-Duct Structure) are introduced in each sub-assembly as a mitigation device. It enables early fuel discharge before the formation of a large-scale molten pool, which has recriticality potential due to large-scale fuel compaction (Suzuki et al., 2014). The feasibility of this upward-discharge driven by the pressurization of the disrupted core has been investigated by utilizing the phenomenological evidences obtained through well-designed experiments. As a complement in order to avoid further recriticality after FAIDUS actuation and thus to consolidate the in-vessel strategy the CRGT of the JSFR has been designed in order to enable fuel donward relocation out of the core. Another approach, investigated in the European project CP-ESFR core design (Maschek et al., 2011), consists in introducing empty pins in fuel sub-assemblies in order to promote axial material relocation out from the core (19 empty pins out of 271). The appraoch adopted in ASTRID was to introduce fully mitigation dedicated sub-assemblies without degrading too much the core performance. Compared to the approaches presented above, where the mitigation ducts or discharge paths are located inside every each fuel assembly, additional research and development are not required for the qualification of the specific fuel assemblies' design. The DCS-M-TTs were imposed to be located mostly at the core periphery (Figure 5) and in a very limited number in the central part of the core.

2.2. Objectives and strategy of mitigation for ASTRID

The purpose of severe accident studies presented in a safety case is to demonstrate that the associated radiological releases outside of the reactor containment are acceptable and that, following any type of accident, the reactor can go back to a safe state. In order to satisfy this objective of limiting the releases, the aim of safety provisions is to keep the integrity of the 2nd safety barrier (main vessel) and the leak tightness of the 3rd safety barrier (safety vessel: additional shell around the main vessel), and thus to reduce the possibilities of occurrence of severe energetic accidents that might affect these barriers. In practice, two temporal phases of the accident event sequences can be distinguished, during which the confinement must be kept:

- the short-term time period during which it is necessary to control the mechanical energy which could lead to a rupture of the confinement, i.e., 2nd and 3rd barriers. This implies to identify and to control the phenomena leading to power excursions at the origin of the maximum released mechanical energy like presented in (Maschek et al., 2018). This neutronic power excursion is governed by the sodium void worth effect, the fuel recompaction, and the recriticality which likely occurs during the secondary phase;

- the longer-term time period during which the relocation and the cooling of the degraded core materials must be promoted in order to lower the risks of recriticality and of breakthrough of the confinement at the bottom part of the main vessel. Regarding this long-term phase, the safeguarding of the confinement implies, in particular, that enough DHR capabilities are maintained and that the core catcher keeps its integrity.

According to the evaluation criterion (mechanical energy release) adopted to assess the natural behaviour of the core on the short-term of the accident course, the studies carried out during the conceptual design stage of ASTRID have shown that the CFV core may not induce significant mechanical energy release during the primary phase of severe accidents. As far as the transition and the secondary phase are concerned, in the majority of the investigated parametric accidental event sequences (Bertrand et al., 2018), the mechanical energy released by fuel vapour expansion is negligible or about the order of magnitude of 10 MJ (Marie et al., 2016b), (Bachrata et al., 2015)). However, for some very unfavourable event sequence evolutions, the mechanical energy released by fuel vapour expansion reaches an order of magnitude of 100 MJ (Bertrand et al., 2018). Despite the fact that this value of mechanical energy should be acceptable versus main vessel loading capabilities, it has been yet decided to foresee provisions aiming at reducing it because one of the goals of the ASTRID safety approach is to avoid situations leading to significant mechanical energy release and to account for event sequence variability and uncertainties on physics. Furthermore, another design goal is to control the course of the accident event sequence as much as possible and thus to control the molten materials relocation. For all these reasons, it has been chosen to implement two types of mitigation devices inside the ASTRID vessel:

- Mitigation tubes (DCS-M-TT) in order to discharge the degraded fissile material from the core during the secondary phase and therefore to limit the likelihood and the amplitude of a potential power excursion;
- An inner core catcher aiming at collecting and cooling core materials in order to prevent the main vessel and its inner components failure and to ensure long-term cooling of the core materials.

The main vessel takes also a part of the mitigation process. The top-down approach used for its design is underlined hereafter. This domain is related to situations presenting core melting which should be taken into account for the design of the reactor, that is, for which some mitigation actions are foreseen in order to fulfil overall safety objectives expressed in terms of radiological releases. First, in this section, the so-called ‘top-down approach’ used for the design of main vessel is presented in sub-section 2.3. The integrity of this main vessel is aimed to be achieved thanks to mitigation devices, i.e., DCS-M-TT and the inner core catcher, whose aim is to reduce its mechanical and thermal loadings. These mitigation devices are designed in the frame of the so-called “decoupled approach”. In this frame,

loading cases are defined independently of a specific event sequence in order to cover unforeseen event sequences and to provide a margin between loadings affected by various uncertainties on physics and the limit of integrity of the considered mitigation device. These loading cases are presented in section 2.4 for the DCS-M-TT and for the core catcher.

2.3. Top-down approach for the main vessel design

The objective of the top-down approach declined for the main vessel design is first presented in this sub-section. Then the assumption used for design calculations are presented and finally some design improvements aiming at reinforcing the vessel mechanical integrity are mentioned. The design methodology is based on a progressive approach aiming at designing the main vessel as the more resistant as possible and without local weak points, through reinforcing weak points of the components indicated in Figure 2. The design is adapted to cope with the functional role of each vessel component as detailed in Table 2.

Function/component	Main vessel	Safety vessel	Slab	DHX	Core catcher
Leak-Tightness	X	X	X (limit the FP transfer outside primary vessel)	X (post-accident cooling)	
Mechanical integrity	X (keep the core catcher support)		X (no colapse)	X (post-accident cooling)	X (retention and cooling capabilities)
Associated criteria	-Maximum plastic defomation -No impact on safety vessel		-Maximum displacement of the slab -Integrity of the plugs and crossing equipments	-Maximum plastic deformation	-Mechanical integrity -Horizontality

Table 2: Functional requirements and associated decoupling criteria for various internal components of the primary vessel important for safety

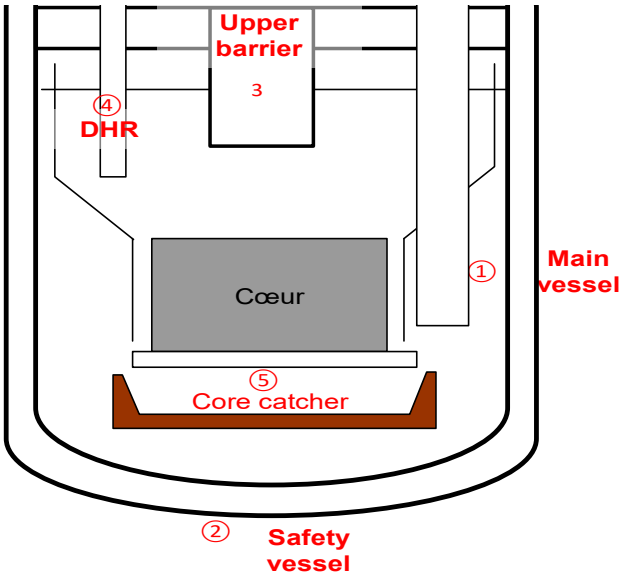

Figure 2 Primary circuit sketch with equipment included in the functional analysis of Table 1

The functional requirements presented in Table 2 are considered to be fulfilled if the criteria provided in Table 2 are respected for each structure. Regarding the top-down approach and the assumptions retained for the design vessel calculation, parametrical studies of high pressure bubble expansions are performed with a fast dynamic calculation code (Europlexus, (Sridi et al. (2016)) taking into account the fluid structure interactions in order to investigate vessel pressure loadings of increasing severity aiming at identifying mechanical weak points on the primary circuit. The severity of the pressure loading applied to the the vessel is increased by increasing the bubble initial pressure. Considering an initial pressure and an intial volume, the presure evolution in the bubble is calculated according to a polytropic law (1):

$$Pv^k = \text{cste} \qquad (1)$$

Where P (Pa) is the pressure inside the bubble, v the volume of the bubble (m^3) and k a polytropic coefficient that is varied in order to perform parametric studies. Moreover, there is a verification of the absence of threshold effect on the loading when calculating the buble expansion and its consequences on each reactor component. This kind of approach permits to study the sensitivity of the design to the mechanical consequences when considering various features of bubble expansion (by varying k) and various initial bubble conditions by variying P at the beginning of the expansion. This bubble is either initially located in the core region to deal with loadings induced by a core material upward dicharge or either located in the cold pool in order to deal with loadings related to FCI under the DCS-M-TT outlets. For each of those parametric calculations, the expansion transient is calculated and is ended when the

structure reaches its maximum deformation. So, by considering the transient history additionally to the structures deformations, the mechanical consequences of the expansion can be featured by the mechanical energy E (J) (equation 2) released from the beginning of the transient up to the reach of the decoupling criteria (Tab. 2).

$$E = \frac{P_f v_f - P_i v_i}{k-1} \quad (2)$$

Where i and f are respectively the initial and final expansion conditions. In general, one says that the vessel is designed for a given mechanical energy value but the relevant information for the design limit deals with the potential loss of integrity of the structure. Design improvements enable to increase the resistance of ASTRID vessel to mechanical consequences. The major design improvements to reinforce the main vessel and its internal equipments were done at an early stage of the design and consisted in: designing a steel slab in order to limit its deformation (pointed out by the number 1 in Figure 3), reinforcing the two lower triple points (number 2 in Figure 3 consisting in the junction between the core support and the main vessel) and incorporating anti blow-out devices on the turning plugs (3 in Figure 3).

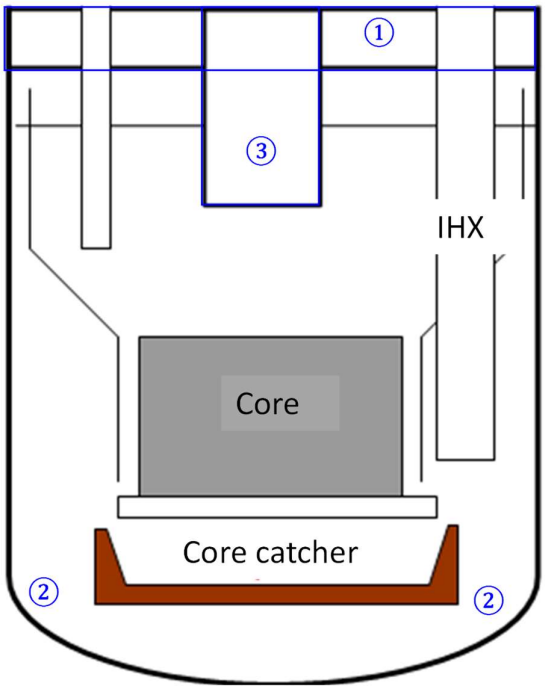

Figure 3 Location of the reinforcements performed in ASTRID main vessel to improve its resistance to mechanical consequences

As far as the DHXs are concerned, several design provisions are envisaged. They are the following: increase of tube thickness (but to a limited extend since the thermal exchanges shoud be degraded by

designing too thick DHX tubes), reinforcement of tubular network by strapping, reinforcement performed at the slab penetration (additional thickness), diversification and redundancy of DHXs location in the vessel.

2.4. Mitigation device design approach

The approach presented here states that mitigation devices are designed as independent as possible of a particular accident event sequence. In that sense, this approach is independant from any event sequences and can be called decoupled approach since degraded states of the core are considered to design mitigation devices. By noticing that, if a severe accident occurs, it means that the control of the reactor has been lost, it is very difficult to predict the value of the loadings that could be induced by a very uncertain and variable event sequence. Moreover, by considering loading cases that are supposed to encompass a wide range of event sequences without retaining a particular one, it offers more warranty to have mitigation devices able to manage unforeseen or forgotten event sequences. Thus, for the preliminary design requirements of DCS-M-TT, a highly common core degraded state is considered, rather independetly from prior events of the accident event sequences. Actually, it can be shown that at the end of the transition phase, the core state is more or less always the same whatever the accident sequence is, since the molten materials are spacially unified under the form of a molten pool. In the same way, regarding the determination of the core catcher design features, it is considered that the whole core materials are degraded and some unfavorable situations, like the failure of some DCS-M-TTs opening, are considered as well in order to have a bounding set of assumptions. Indeed, in such a situation the pathways available to extract the fuel from the core region are reduced.

After a preliminary design of the main vessel and mitigation devices (DCS-M-TT, core catcher), the assessment of the design adequacy is done by investigating some loadings induced by various realistic accidents sequences, providing that there is a wide margin between loadings induced by accident sequences on mitigaction devices and their design limit. In the following sub-sections, the decoupled approach is presented as applied for the design of the DCS-M-TT and of the core catcher.

2.4.1. DCS-M-TT design process and assumptions

The general scheme of the location of the DCS-M-TT is presented in Figure 4 and Figure 5. The geometry of each DCS-M-TT, presented on Figure 6, should promote material relocation downwards to the core catcher as fast as possible in addition to the possible but more limited mass relocation into the CRGTs (the free volume in their feet is very low). To do that, these DCS-M-TT must have a reduced cross section in their upper part and cross the diagrid and the strongback in order to let open the material flow path towards the core catcher.

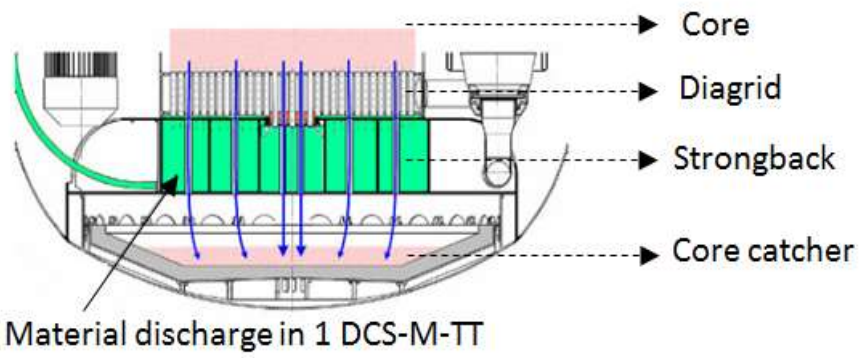

Figure 4 Vertical cross-section of the cold pool of ASTRID and sketch of the DCS-M-TT

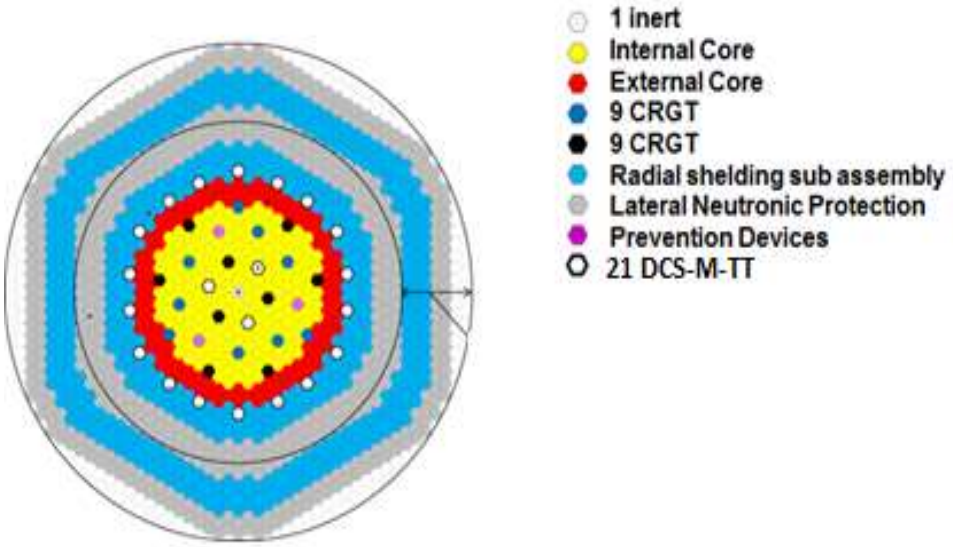

Figure 5 Horizontal cross-section of the CFV core (CRGT stands for control rod guide tube; DCS-M-TT stands for transverse tube mitigation devices)

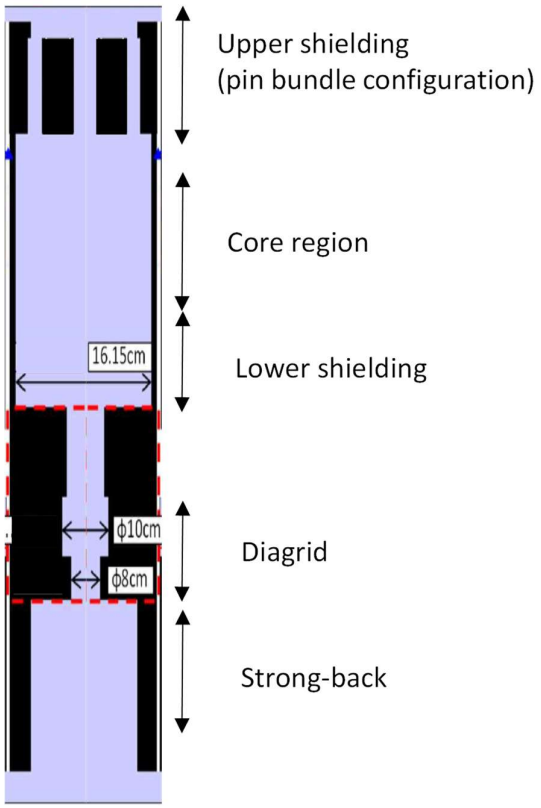

Figure 6 Vertical cut-set of a DCS-M-TT

A lot of sensitivity studies have been performed with SIMMER (Yamano et al., 2003) and with the fast-running tool MARINa (Marie et al. 2016b) on the highly common degraded state presented in (Bertrand et al., 2018) in order to explore adjustable design parameters of DCS-M-TT. SIMMER is an Eulerian, two-dimensional multi-velocity-field, multi-phase, multi-component, fluid-dynamics code. It is coupled with a fuel-pin model and a space and energy dependent quasi-static neutron kinetics model (16 energy groups have been used for the studies presented in this paper). The threedant module has been used for neutron physics in 3D calculations and the twodant one in 2D calculations. SIMMER can handle material movements in a molten pool once the hexcan are molten. More details on SIMMER are available in (Yamano et al., 2003). The CFV core radial discretization has been made in SIMMER two -dimensionnal calculations according to the actual successive rings of the sub-assemblies of the core starting from the core center (11 rings for the whole core). MARINa is a CEA home made fast-running calculation tool, solving balance equations (mass, mometum and energy) in the molten pool encompassing fuel and steel. It includes a neutron physics point kinetics module taking into account the axial flux profile modification associated to material movements. The reactivity evolution calculated by MARINa considers various effets expected in a molten pool configuration (mixing/segregation of steel, material extraction from the pool, temperature, etc.). More details on MARINa are presented in (Marie et al., 2016b). These parametric studies have enabled at investigating the whole range of reactivity

effects that can lead to a power excursion during the transition and secondary phases. As an illustration, a spatially coherent decantation of steel by using a maximized decantation speed has been investigated. The same kind of approach has been used for the study of other reactivity effects. Penalizing assumptions have also been retained for studying parameters delaying[3] the fuel extraction from the core region that stops power excursions. The main results of these parametric studies indicated in particular that the upper and lower DCS-M-TT cross section (in the diagrid elevation) have a minor influence on the fuel mass extracted from the core (Bertrand et al., 2018). It also has been shown that the fuel draining through the DCS-M-TTs leads to the insertion of a very large negative reactivity inside the core as soon as it becomes prompt-critical.

At the beginning of the design, the number and the location of DCS-M-TT have been defined to limit the number of DCS-M-TTs inside the inner core at 3 because they are very penalizing in terms of core performance. The number of DCS-M-TTs at the core periphery is more adjustable but with less than 18 tubes, the "spatial overlapping" able to prevent radial molten material propagation towards the internal storage could not be sufficient. Conversely, parametrical calculations have indicated that increasing the number of DCS-M-TT devices beyond 18 inside the peripheral region of the core does not favour the kinetics of the material relocation (see Figure 6) neither the final total amount of relocated mass. However, left hand side of Figure 6 shows that with the three DCS-M-TTs implemented into the inner core, the fuel extraction begins significantly earlier than without them, therefore enabling an early mitigation of possible secondary power excursions. Moreover, in case of secondary power excursion induced by steel decantation in the molten pool of the upper fissile zone, the molten materials of inner core are partly ejected upwards and partly relocated downwards onto the core catcher in case of non-obstructed PNS. If the PNSs are obstructed by frozen materials ejected during the accident, these latter are only relocated on the core catcher in several seconds. On right hand side of Figure 6, the mass difference between the blue curves and the red curves corresponds partly to upwards-ejected mass and to mass remaining into the core region[4].

[3] For instance, the full thermal erosion of a DCS-M-TT wall is required before initiating the material draining into it.

[4] The calculated transient begins at time = 0 s. The plot corresponds the mass arriving onto the core catcher. The time delay of 1.5 s is due to material transit time into the DCS-M-TTs.

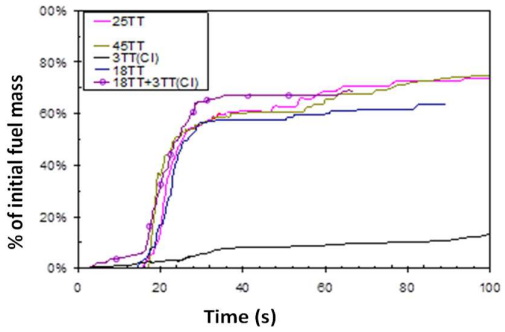

SIMMER calculations results: impact of the DCS-M-TT (TT) number on mass fuel relocated onto the core catcher; (TT (CI) stands for the number of DCS-M-TTs in inner core)

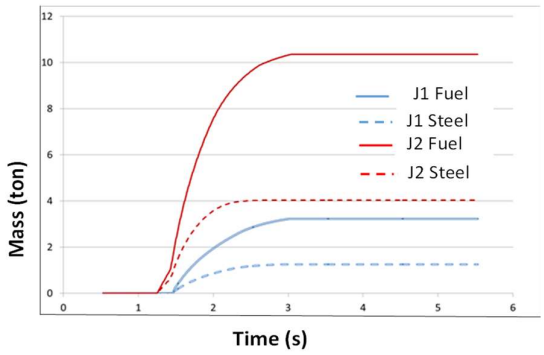

Analytical tool calculation results: impact of upper core fluid cross section blockage on molten material relocation onto core catcher of inner core relocation in case of secondary power excursion (J1: no blockage; J2 blockage)

Figure 6 Parametric calculations results on DCS-M-TT performed starting from the general common core degraded state: material mass relocated onto the core catcher (time scales of both sides of figure are different because left hand deals with nominal constant power and whole core consideration whereas right side deals only with inner core and associated DCS-M-TT behaviour in case of secondary power excursion)

Figure 7 shows that the reactivity and power evolutions during the accident are strongly limited by the presence of DCS-M-TTs inside the core. As a result, the thermal energy deposition and thus the mechanical energy released by fuel vapour expansion does not exceed the order of magnitude of 10 MJ with DCS-M-TT whereas it can be one order of magnitude larger without DCS-M-TT as shown in Figure 10.

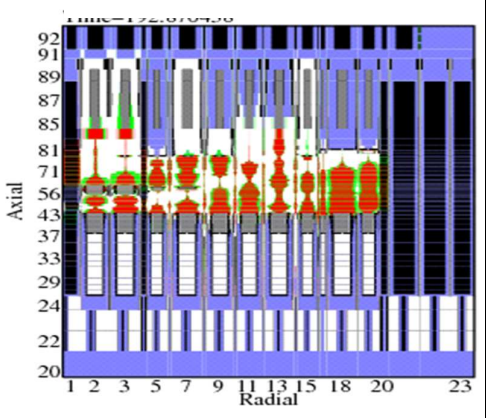

Core state after secondary power excursion (no DCS-M-TT)

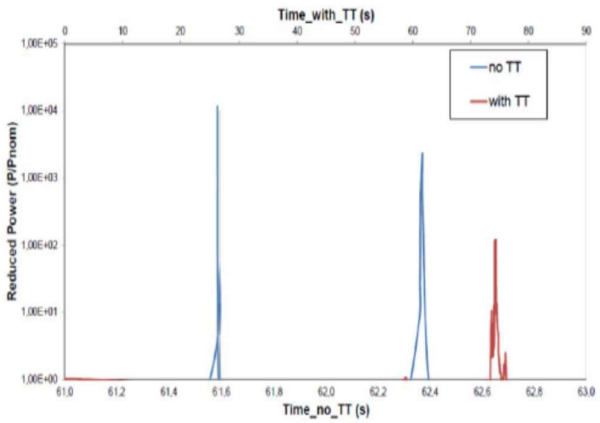

Normalized power evolution during secondary phase with and without DCS-M-TTs (time zoom on power increase)

Figure 7 Core state after first power peak (left hand side; blue: sodium; white: vapor; red: molten fuel; green: molten steel) and normalized power evolution without and with mitigation devices (right hand side) for ULOF whole scenario calculation

In the case without DCS-M-TT calculated with SIMMER III, a super-heated fuel mass of about 26 t is obtained inside the core region whose average temperature is about 4500 K. These results have been

used as input parameters of the DETONa physical parametrical tool (Manchon et al., 2017) which calculates the mechanical energy release transient by solving the mass, momemtum and energy equations in the expanding fuel vapor bubble and in the cold surrounding sodium. The nodalization is done in a multi-0D spherical zone domain (liquid fuel, vapor fuel, sodium and argon). The mechanical energy is about 300 MJ. Despite this value has been obtained with some conservative assumptions like the absence of vessel structure deformation for instance, some other assumptions are not conservative. This is the case of the absence of fission gas inside the expanding bubble. So this expansion mechanical energy amount of 300 MJ should only be considered as an order of magnitude. In the case with DCS-M-TTs calculated with SIMMER III, the molten mass in the core is equal to 18 t and the corresponding fuel average temperature is about 3500 K, that is under its saturation temperature at the primary circuit pressure. As a result, in this calculation, the mechanical energy released by fuel vaporization is equal to zero thanks to the DCS-M-TT.

2.4.2. Core catcher loading cases

This sub-section is limited to assumptions aiming at defining cases related to liquid jet transients retained to calculate thermal loadings inducing core catcher erosion due to molten jet impingement. The main data, needed in order to assess the risk of failure of the core catcher by jet impingement, deals with: the mass of materials relocated onto the core catcher by each DCS-M-TT, the material composition and the temperature of the jet impacting the core catcher. All these data have been evaluated and are specified hereafter.

- Radial zone of molten core collected by DCS-M-TT by assuming three bounding situations

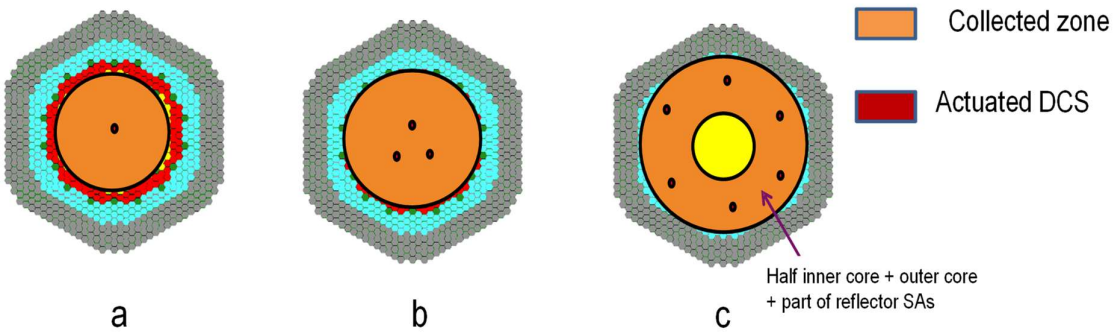

Figure 8 Loading case configurations defining the radial zone of molten core collected by each DCS-M-TT

In order to have an idea of the material mass flow rate in each each DCS-M-TT, it is necessary to assess the mass collected by each tube. Three different cases, called a, b and c, have been proposed in the frame of the ASTRID pre-conceptual design (Figure 8) by considering various potential degraded core states.

- Case « a », base case with power excursion:

In this case, in the frame of the decoupled approach, it has been considered by starting from the general common core degraded state representative of the end of the transition phase (Bertrand et al., 2018)) that only one DCS-M-TT is operational. In this state, only the inner core is totally molten and it is assumed that due to core region pressurization, as soon one DCS-M-TT is open, all the inner core molten materials are relocated through it. Moreover, ULOF calculations and scenario calculations from a degraded state (done with SIMMER and MARINa, (Bertrand et al., 2018)) have shown that 25 tons of fuel at the maximum, are relocated during the early discharge: including 13 tons from the inner core and 12 tons from the outer core. Furthermore, SIMMER and MARINa calculations have shown that fuel and steel are relocated together and that the mass of steel relocated is about half of the fuel mass. A physical upper bounding temperature is proposed for each kind of relocated material. It is its boiling temperature. So as a result, the first loading case proposed to be investigated corresponds to molten materials relocation through one DCS-M-TT located inside the inner core of 13 tons of fuel, 6.5 tons of steel with a jet temperature of 3100 K (approximately the boiling temperature of the fuel/stainless steel mixture).

- Case “b”:

In this postulated case b, we consider a longer transient than in case a owing to the absence of large recriticality corresponding to scenarios enabling the total fuel mass (except lower fertile plate) to be relocated on the core catcher. Because the transient is longer, we can envisage separated relocations between fuel and steel including the relocation of the medium fertile plate of the CFV core (Bertrand et al., 2016). So in this situation, providing that the transient is longer than in a case without any pressurization of the core region[5], we assume that all the DCS of inner core (3 DCS-M-TT) are operational and opened and that the jet features are the following: 25 tons of fuel and 12,5 tons of steel. Moreover, 2 jet configurations are considered:

- A fuel/steel mixture jet at a temperature of 3050 K;
- A pure fuel jet followed by a pure steel:
    - Fuel jet temperature of 3050 K

[5] In case of a pressurized core region, core material can be fast discharged by the first tube open, by bypassing the others that could not yet be open before the end of the discharge and by being pushed by the pressure. On the contrary in a non-pressurized case, the materials stay longer into the core and all the tubes can be opened during the discharge.

- Steel jet temperature of 2000 K (result from molten pool analytical calculations performed with MARINa).

- Case “c”:

Finally case c is not a dimensioning loading case versus jet impact. Indeed, in this case a larger number of operationnal and opened DCS-M-TT is considered.

3. **Verification of the efficiency of the DCS-M-TT**

Preliminary assessment of the DCS-M-TT efficiency is presented in this section. This efficiency verification calculations are performed for the whole core since the efficiency of DCS-M-TT is related to reactivity shutdown governed by fuel discharge. The verification approach is introduced before the calculation presentation.

3.1. *Verification approach*

The approach adopted to design the DCS-M-TTs has been presented in the previous section of this paper. The main applied design principles were aimed at getting rid as far as possible of accident event sequence dependency (the so called ‘decoupled approach’). Once the mitigation devices are featured at best, their efficacity is assessed by calculating accident event sequences. Verification studies are carried out to check if there is a substantial difference between the loss of integrity limit (this loss can be expressed through a relay criterion called “criterion” in Figure 9)) of the considered component (main vessel or core catcher) and the loading induced by the most likely expected event sequence. This latter is assessed through a mechanistic calculation (SIMMER coupled with a fast dynamic code). Additionally, the spreading of this loading around its best-estimate result is assessed through statistical calculations that have to demonstrate that the risk to exceed the criterion is low enough. Finally the combination of the difference between the best-estimate calculation and the criterion, and, the risk that the loading exceeds this criterion gives the margin between the loading and the design (or safety) criterion (see fig. 9).

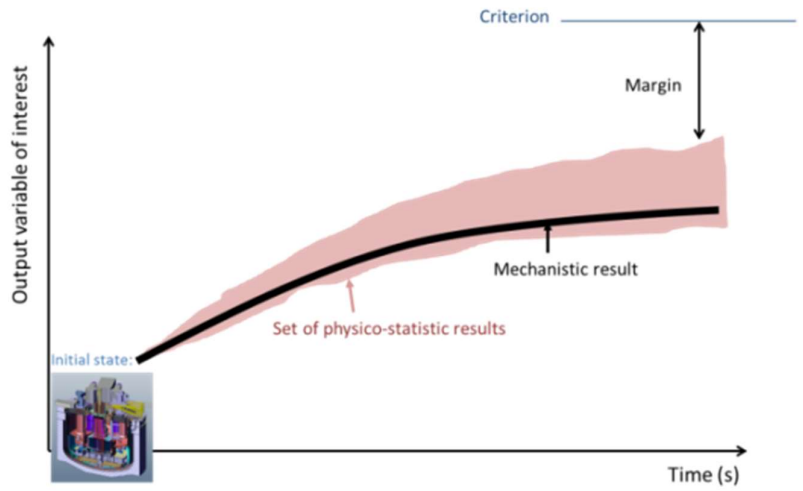

Figure 9 Combination of mechanistic and physico-statistical calculations for margin assessment: evolution of the variable associated to the criterion for the best-estimate case and set of fast-running tool calculation results representing the scenario variability due to uncertainties (pink zone encompassing mechanistic best-estimate calculation result)

3.2 Whole core calculation insights

Whole core calculations of the secondary phase relocation process have been performed by CEA with MARINa in order to assess the variability of the secondary phase evolution versus main uncertain parameters and versus DCS-M-TT design parameters (geometry, number). Statistical calculations are performed as a complement of BE calculations (as indicated in Figure 9) in order to investigate the main governing parameters of the relocation process and the spread of the results. They are presented in section 3.2.1. Moreover, whole core mechanistic BE calculation results with SIMMER-IV with a 3D modelling are displayed in section 3.2.2. and 3.2.3 in order to compare ULOF consequences respectively without and with DCS-M-TT.

3.2.1. Study of DCS-M-TT efficiency at the beginning of the secondary phase

Some physico-statistical studies have been performed (Marie et al., 2016a) by means of the MARINa tool by starting the calculations from the general common core degraded state presented in by Bertrand et al. (2018). The aim of these studies was to investigate the variability of the secondary phase evolutions when various assumptions are envisaged and taking into account some uncertain parameters of physic models. Among others, the impact of the behavior of the DCS-M-TTs on the reactor state of the secondary phase has been studied. About 20 input variables of MARINa have been probabilized. They are mainly related to:

- the fuel and steel configurations in each fissile zone (mixed or segregated);
- their temperature;
- the leak-tightness/or not of the upper shielding (plugged/unplugged) and the presence/or not of a crust above the pool;

- the number of DCS-M-TTs operating;
- the mixing time/decantation time of steel and fuel;
- the nature of the opening criterion of DCS-M-TTs (mechanical or thermal);

8000 simulations have been realized in order to cover 4 various initial configurations (mixed/separated materials in the upper fissile zone and upper shielding plugged/unplugged). Those calculations highlight that a power excursion occurs in only 8% of the simulation cases and that molten materials are ejected above the core in only 18 % of these cases. The average final relocation spots of the fuel and of the steel are presented in Table 3.

Table 3 Average relocation spot of fuel and of steel of the ASTRID inner core

	Above core	Core catcher	CRGTs foot	In core region
Fuel mass fraction (%)	9.5	45	3.5	42
Steel mass fraction (%)	11.5	51	3.5	34

The general conclusions that can be drawn from these calculations are the following:

- secondary phase evolution is mainly governed by the behavior of the molten materials located inside the upper fissile zone;
- the decantation of the upper fissile pool inserts a large reactivity that leads to a power increase and to the heating of the molten materials, possibly to their boiling and to their upward ejection;
- the DCS-M-TTs enable to reduce the material mass remaining into the core but cannot enable to prevent from prompt-criticality neither from the ejection of a part of the materials above the core.

Generally speaking, these studies have confirmed that the implementation of DCS-M-TTs in the inner core reduces the risk of prompt-criticality and increases the material mass relocated onto the core catcher (Figure 10). Moreover, the studies have underlined the necessity to accurately model the upper pool decantation and the possibility to have a plugged upper shielding due to relocated materials during previous phases of the accident. More precisely, transient evolutions (including mechanical consequences) and above everything the final material distribution can vary a lot depending if whether or not materials can be ejected above the core.

In conclusion, MARINa calculations done by varying several uncertain parameters have shown that DCS-M-TTs enable to relocate about 50 % of the fuel material onto the core catcher even if they do not prevent the occurrence of a power excursion in about 10 % of the transients calculated over the large number of simulated situations (8000). As the other step of the approach presented in section 3.1, two mechanistic calculations have been done and are presented in the next section for a ULOF transient.

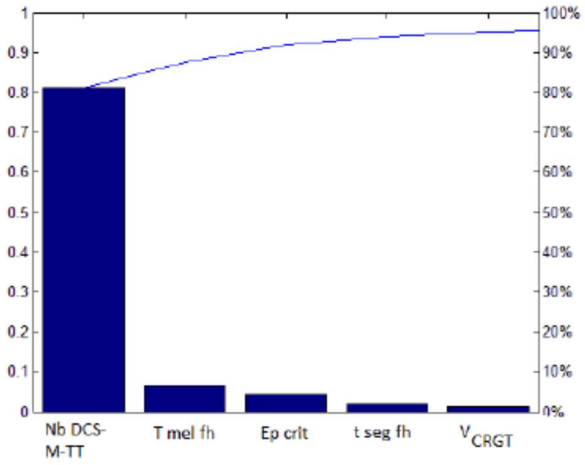

Figure 10 Sensitivity index of various input parameters on relocated mass on core catcher (Nb DCS-M-TT: number of DCS-M-TT; $T_{mel\ fh}$: upper mixed fissile pool temperature; Ep_{crit}: critical thickness of TT leading to its opening; $t_{seg\ fh}$: segregation time of upper fissile pool; V_{CRGT}: CRGT foot free volume)

3.2.2. SIMMER-IV ULOF calculations

ULOF calculations have been performed at CEA with SIMMER IV since 2016. The status of these calculations is synthetized here by focusing on the efficiency of DCS-M-TTs. The first part of this section is dedicated to the presentation of a core calculation with the CFV core without DCS-M-TT whereas the second part of the section is dedicated to calculations performed with DCS-M-TTs into the core (Bachrata et al., 2019).

-ULOF calculation without DCS-M-TT

The flow rate is imposed at the core inlet in order to obtain a ULOF with a primary flow rate halving time of 10 s. The boiling onset leading to reactivity oscillations begins around 30 s in the inner ring of SAs of the external core. When the liquid mass of fuel into the core reaches about 25 % (at 111 s), a first power excursion occurs. Due to the Doppler Effect and to the molten materials dispersion within the core region this first power peak ends. However, this first power peak induces further fuel melting and associated fuel axial compaction. As most of the fissile mass remains inside the core, a second power excursion occurs leading to a power peak reaching 1500 times the nominal power. The core molten mass fraction after this peak is about 45 % of the total fuel inventory. The average temperature of the fuel is equal to 3500 K.

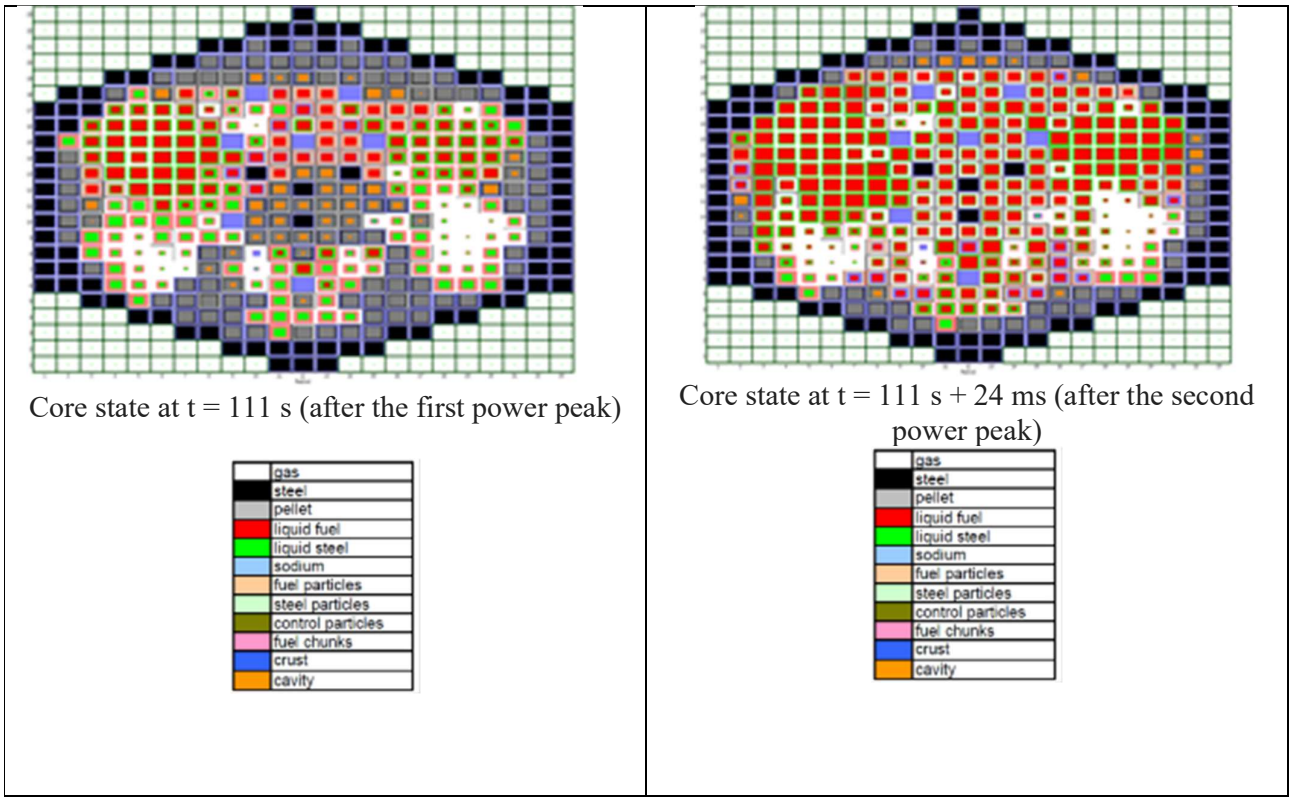

Figure 11 Horizontal cut-sets of the core after the two power peaks

3.2.3. ULOF calculation with DCS-M-TT

The core and main vessel nodalizations including DCS-M-TTs used for this calculation are presented in detail in (Bachrata et al., 2019). The DCS-M-TTs are covered by an upper shielding of "removable type" associated to a fluid cross section of 35 % of the whole section. The diameter of the tube is restricted to 80 mm at the diagrid elevation. When the pumps are shutdown, thus initiating the ULOF transient, the flow in all the DCS-M-TTs goes upwards because of the decrease of the pressure excess of the hot plenum due to a pump head decrease. Compared to the calculation performed without DCS-M-TT, all the events of the transient related to the SA degradation are shifted of about 10 s in the simulation (Table 4). This can be explained by a slightly higher flow rate with DCS-M-TT than without during the pump rundown.

Table 4 Comparison of the main transient events with and without DCS-M-TT

	Instant (s) No TT	Instants (s) With TT
Boiling onset	29.8	33.7
Start Clad melting	43.3	52.2
Fuel	43.3	52.2
Hexcan wall melting	50.2	61.0
Power excursion	111	127

At 110 s, only 8 % of the fuel is degraded compared to 25 % in the calculation without DCS-M-TT. A power excursion occurs at 127 s once about 19 % of the fuel in the core is degraded. As indicated in Figure 12, one of the peripheral DCS-M-TT opens at 128 s, that is, one second after the power excursion. Then, 0.2 s later, one of the DCS-M-TT located inside the inner core opens. After one second, 3 peripheral DCS-M-TT are opened. However among the 3 DCS-M-TT of the inner core, only one contributes to the discharge during more than 7 seconds. It means that the assumptions retained for the loading cases related to the core catcher design are relevant because the DCS-M-TT inside the inner core are not opened at the same time (cf. section 2.3.2). Therefore the jet discharge by the first single opened DCS-M-TT has a long duration and has time erode the core catcher. After the opening of the DCS-M-TTs, the reactivity decreases and reaches a very large negative value compared to the case without DCS-M-TT (Figure 13). That ends the transient.

In conclusion, about 23 % of the fuel inventory is discharged onto the core catcher in 19 seconds. Moreover, the power peak is only about 250 times the nominal power when the core is equipped with DCS-M-TT instead of 1500 times in the case without DCS-M-TT, thus showing the efficiency of these tubes for this best-estimate calculation. The efficiency demonstration of mitigation device has to be consolidated by decreasing uncertainties and improving some models in order to better simulate the accident sequences, both in SIMMER and in fast-running tools. This is why a PIRT has been developed in order to hirachize R&D efforts in the future. This PIRT is presented in the next section.

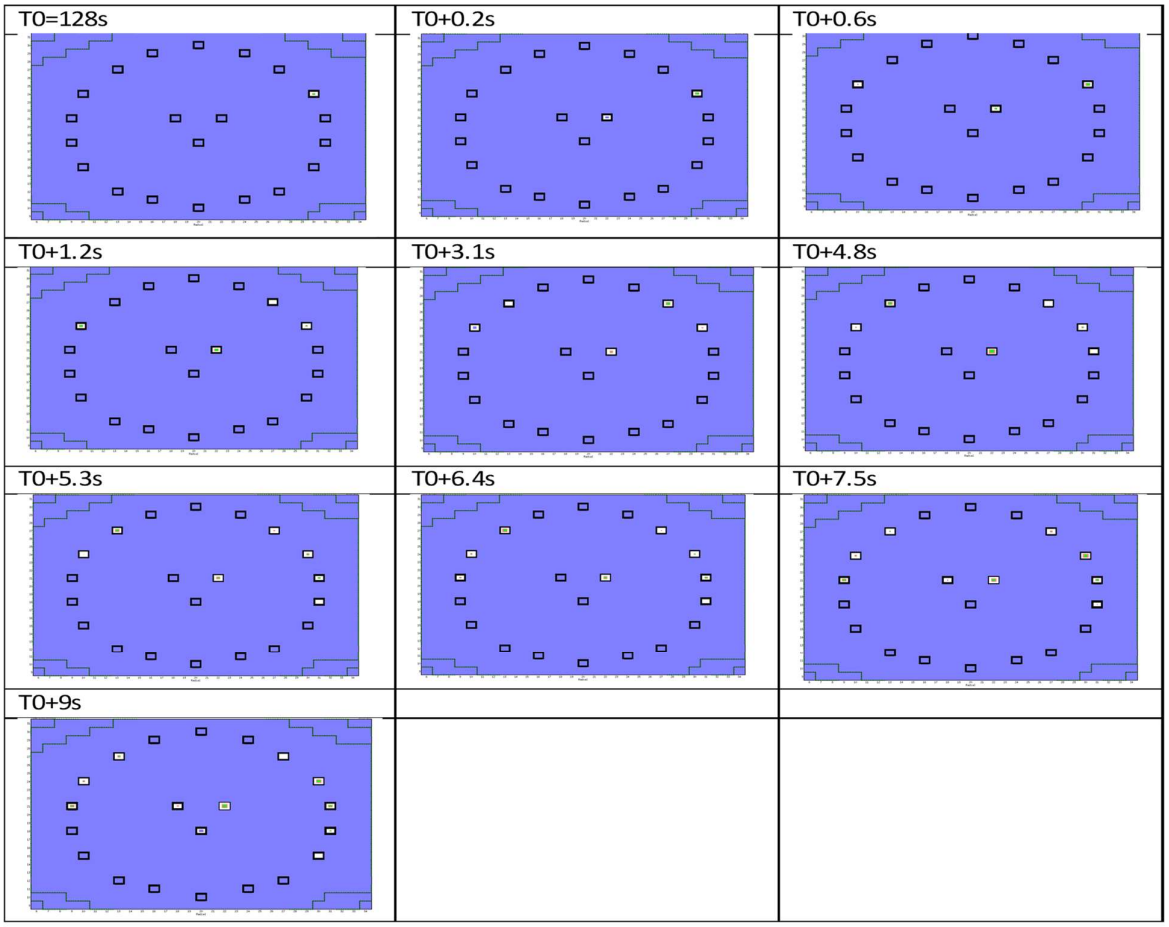

Figure 12 History of the opening of DCS-M-TT

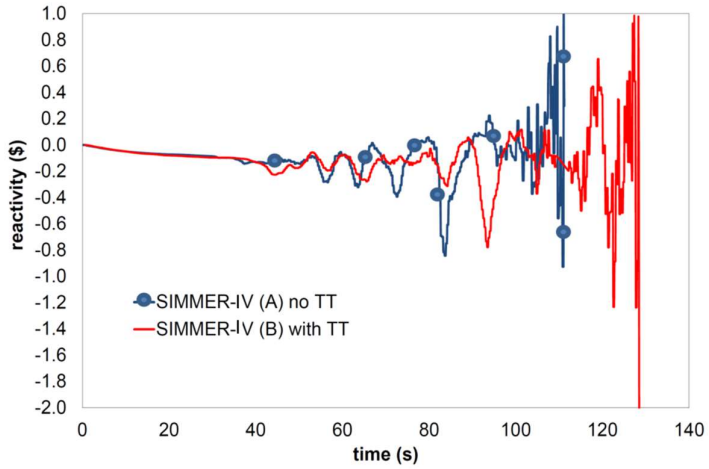

Figure 13 Comparison of the reactivity evolution without (no TT) and with (with TT) DCS-M-TT

4. Generic event sequence investigation and PIRT (illustration for ULOF)

The objectives of this generic investigation is to establish a methodology and a frame for the investigation and the physical understanding of SA (severe accident) sequences. Two kinds of event tree (ET) or event chart are described. The first one is a generic ET (GET). This generic event tree illustrates general event evolution and their consequences. The second one is a phenomenological event chart (PEC). PEC describes relationship among key physical phenomena and event sequences in each event on GET. Furthermore, PEC is useful for identifying important parameters and required modellings in simulation tools. Several GETs, which express general event sequences, and PECs, which closely link with the evaluation contents, are incorporated to the paper hereafter for the ULOF event sequence. Core states described in the GETs are characterized by dominant phenomena and their relations with "headings", i.e., branching points of GETs (Fig. 14) will be analyzed thanks to PECs. Physical phenomena represented by PECs will be assessed with fast-running tools than can be easily parametrized (see for instance: Droin et al., 2017). PECs can simulate a time period of an event sequence (Droin et al., 2017) or can simulate the core and reactor evolution by starting from a degraded state of the core (Marie et al., 2016b).

Figure 14 shows framework of ULOF accident phases and their relation to the headings of GETs and PECs. The accident phases presented in Figure 14 enable to separate various GETs according to successive core configurations. The primary phase corresponds to events occuring in an overall core geometry which globally remains the same as in nominal operation: sodium boiling, fuel pin degradation and material relocation occur in SAs that are isolated from each other, that is, at a stage of the accident where the hexagonal tube surrounding the SAs (hexcan) have not failed. Then starts the transition phase during which the degraded zones begin to radially expand up to a phase where the degraded core consists, in average, in a large molten/degraded volume. This phase is called secondary phase of the accident. Finally, the last phase of the accident is associated to a core neutronic configuration, resulting from molten material degradation and relocation, which, is sub-critical and coolable. This phase is called post-accidental cooling phase. There is another phase that might occur whenever during the other phases except during post-accidental cooling phase: this is the expansion phase. This latter phase might occur as soon as some core materials and/or sodium are super-heated compared to their saturation temperature at their actual pressure. In such situations, the super-heated materials are vaporized at a high pressure and the formed vapors expand, thus releasing some mechanical energy.

	Primary phase	Transition / Secondary phase						Post-accidental cooling phase
		Short term core materials motion (pool formation)			Short term consequences		Long term relocation	
		SA-scale pool	Medium scale pool	Whole core pool	Energetic core expansion into upper plenum	Large scale FCI in lower plenum		
Heading of Generic Event Trees	Energetics due to coherent materials motion	Severe re-criticality due to axial compaction	Severe re-criticality due to axial/radial compaction	Severe re-criticality due to axial/radial compaction	Failure of RV	Failure of CC due to massive molten jet attack	Long term relocation &cooling	Long term cooling
			Massive Fuel discharge via internal TT	Massive Fuel discharge via peripheral TT	Failure of DHRS	Failure of RV		
					Sodium release due to failure of reactor roof seal	Failure of DHRS and/or CC		
Elements to be defined in Phenomenological Event Charts	Coolant boiling and Fuel pin failure, associated reactor power / flow ratio change	Degraded core axial motion, (formation of bottled-up configuration), associated reactor power change	Degraded core axial/radial motion, TT and CRGT wall failure, fuel discharge, associated reactor power change	Degraded core axial/radial motion, TT and CRGT wall failure, fuel discharge, associated reactor power change	Energy conversion during core expansion, Structural response	Energy conversion during FCI, Structural response Molten jet break up, jet attack	Long term relocation &cooling for core remaining fuel	debris bed cooling, thermal load on the core catcher

Figure 14 General event sequence and consequences

4.1. Phenomenological event chart (PEC)

The PEC presented in Figure 15 indicates the thermal-hydraulic and neutron physical phenomena that can occur during a ULOF starting from pump trip and ending at the end of material relocation. As indicated on this PEC, the key parameters depend on the flow rate redistribution between SAs and on the possible occurrence of a power excursion. Then at the end, depending on these parameters, a whole core melting might happen and mechanical energy might be released. All the various phenomena expected during the ULOF transient are simulated in mechanistic tools like SIMMER (Yamano et al., 2003) but also in physical parametrical tools with a short execution time (Herbreteau at al. (2017), Marie et al. (2016), Manchon et al. (2017)). Thanks to these latter, it is possible to assess, for a large range of event conditions, the event evolution.

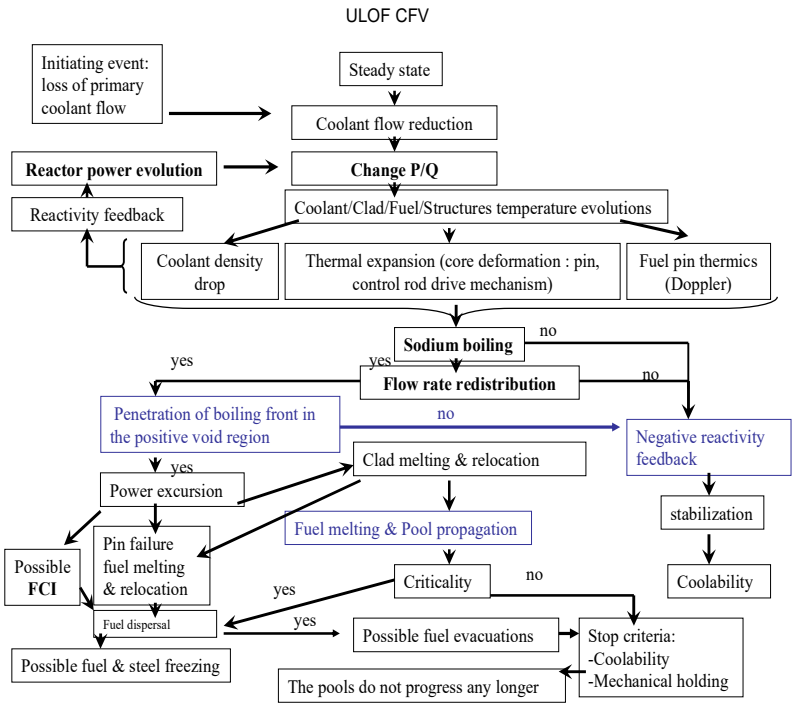

Figure 15 Phenomenological event chart (PEC) for ULOF

4.2. Generic event trees (GET)

An ULOF generic ET illustration is displayed in Figure 16. Basic event sequence is as follows: Primary phase→Transition/Secondary Phase (short-term relocation) → long-term relocation →Post-accidental cooling phase. No possibility to reach energetic sequences in the primary phase of the CFV[6] core is expected (Bertrand et al., 2018). Corresponding time scale of each phase of the accident is from several tens of seconds up to a few minutes. Results obtained regarding short-term relocation influence transition to long-term relocation and final results. Time scale of process of these accident phases is of few minutes up to few hours or longer period. In post-accident cooling phase, only relatively short-term (i.e. for few hours up to few days) is presently evaluated. However, longer term (over few years) coolability should be also considered. In the process of relatively short-term period, coolability for various materials relocation conditions which is obtained as a result of upstream accidents phases will be considered. In order to judge branching for each heading of GET, it is necessary to identify dominant phenomena at each accident possible evolution change (GET bifurcation) through the simulation of phenomena described by the PEC associated to the GET bifurcation. Important parameters which influence the event evolution towards one branch of the GET or towards another should be identified. For this purpose, methodological tools such as PIRT may be useful (see next sub-section). Then parametric analysis which evaluates sensitivity of safety important parameters to various physical

[6] CFV core: low void worth core avoiding to insert reactivity due to liquid sodium disappearance from the core.

phenomena is conducted. Here, construction of best-estimate base event sequences or conservative ones in a deterministic way is intended through these analysis and evaluation, rather than evaluating branching probability of GETs. This probability assessment could be performed in a next stage of the studies.

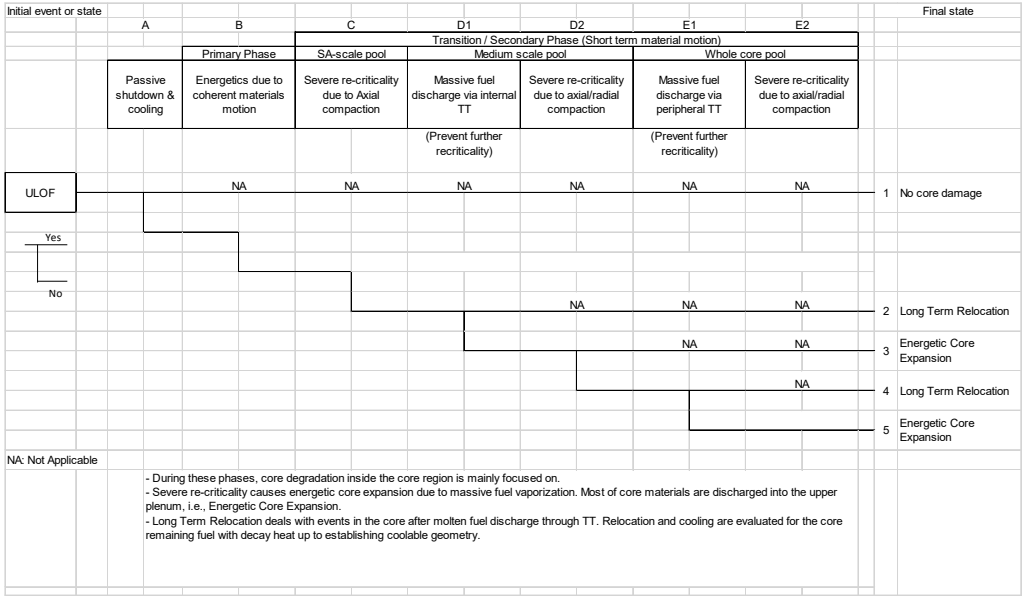

Figure 16 ULOF Generic event tree Primary phase and Transition / Secondary phase (Short-term relocation)

4.3. Phenomena identification and ranking table for ULOF (PIRT)

According to the studies for the future, a PIRT has been developed for the structuration of the ULOF sequence in various temporal period. In section 4.3.1, the methodology adopted to build the table is presented. Then, on the basis of some existing PIRT's, the organization of the event sequences, the figures of merit and the phenomena retained for evaluation of ASTRID ULOF are described in section 4.3.2. As a prospect, the ranking of the importance and of the uncertainties of various phenomena according to their respective figure of merit will be done to orientate future R&D tasks to be shared between France and Japan.

4.3.1. Objectives of a PIRT and general methodology for its elaboration

The objective of a PIRT dedicated to severe accidents is to identify phenomena that are both of high importance for safety and associated to a high level of uncertainties (OECD, 2018). These phenomena deserve further comprehensive analysis and/or experimental studies. PIRT result analysis should enable

to make a large consensus on severe accident issues on which large uncertainties subsist (EURSAFE, 2005) in order to:

- Improve reliability on event sequence analyses by reducing the uncertainties to manage when considering coupled phenomena and successive stages of events;

- Provide a structure to the R&D programme needed to reduce uncertainties.

In a first stage of the PIRT elaboration, it is necessary to split the accident sequence into successive time periods. This time period separation aims at gathering consistent phenomena (in terms of time frame and scale) versus the same figure of merit. A figure of merit or evaluation criterion consists in a physical quantity that is relevant for various phenomena importance (importance is defined hereafter).

As far as the ranking of phenomena depending on their importance is concerned, the following indications can be kept in mind:

- High importance phenomena: it has a high impact for safety (high risk: i.e., high consequence and high probability (OECD, 2018)). Therefore, it should be assessed with high accuracy in computational tools and should be investigated through experimental programmes;

- Medium importance phenomena: they have a moderate impact for safety but experimental studies and analytical modelling are required anyway;

- Low importance phenomena: they have only a small or no impact. Therefore, a rough modelling is sufficient.

Regarding the ranking of the knowledge level of phenomena**,** some orientations presented below can generally be found in the literature (EURSAFE, 2005)):

- Phenomena with good knowledge means that calculation tools are validated on a large experimental data base and that there are affected by a low level of uncertainty;

- Basic knowledge of the phenomenon but poor knowledge in some ranges of parameters and some uncertainties in particular when extrapolating to reactor scale;

- Poor knowledge of phenomena and very few experimental data. No validated model exists.

4.3.2. Application of general principle to ASTRID and proposal of specific issues

The split of ULOF sequence into various time periods has been done according to the headings of generic even trees (GET) has been presented before in this section. As a result, we have the following accident phases: primary phase, short-term relocation in transition and secondary phase, long-term

cooling and relocation phase and expansion phase. The figure of merit (FoM) associated to each accident phase is presented hereafter.

During the primary phase, one important event bifurcation between core melting prevention and core melting occurrence is the sodium boiling onset. Therefore, the quantitative FoM enabling to assess if 'the core could be degraded' are the maximum sodium temperature, quality or average sodium void fraction in the subassemblies (SAs). The second FoM of interest regarding the primary phase is 'the feature of a possible power excursion'. Therefore, the corresponding proposed quantitative FoMs are the core stored energy and the core SA failure fraction. Regarding the short-term relocation in transition/relocation phase, the potential for mechanical energy release during the short-term relocation phase is related to the following FoM: 'the core stored thermal energy' and to 'the fuel mass inventory in the core region' at the end of this phase. The phenomena taken into account regarding the expansion phase are aimed at assessing the core materials and sodium expansion consequences. These consequences can be associated to 'structure loadings and deformation'. Therefore, the main relevant generic FoMs leading to structure (vessel and its inner structures, core catcher) loadings are: 'sodium kinetic energy', 'argon compression work', 'impulsion' (integral of pressure versus time), 'expanding bubble expansion work'. Finally, for the long-term cooling and relocation phase the main FoMs deal with the 'distribution of the core materials' (the remaining part in the core region and the relocated part onto the core catcher) and in particular of fuel. This distribution defines the possibility to cool down them without any further material progression and to keep a sub-critical state.

5. **Conclusions**

SFR severe accidents investigations carried out for ASTRID reactor are synthetized in the body of this article. The first part of the paper is devoted to mitigation strategy and to preliminary design of mitigation devices. The design has been carried out by defining possible loading conditions as decoupled as possible from a particular event evolution. This enables to provide a robust design covering unforeseen event evolution, uncertainties on physics and on event evolution as well as unpredicted event evolutions. Such a design strategy has been applied to DCS-M-TT whose aim is to reduce core reactivity in order to prevent from large mechanical loading on the reactor vessel and on its inner components. Moreover, considered loading cases for core catcher and main vessel have been presented as well. Parametrical studies performed on DCS-M-TT have led to implement 3 TTs in the inner core and 18 TTs at the core periphery. Furthermore, ULOF sequence calculations have shown that the presence of DCS-M-TT leads to mechanical energy decrease of about one order of magnitude compared to a core without DCS-M-TT. Indeed, in case of ULOF, mechanical energy released by fuel vapor expansion would not be significant, that is to say at the maximum equal to several 10^{th} of mégajoules.

Among the three accident sequences (ULOF, UTOP and USAF) able to initiate a whole core melting situation, physical phenomena occurring during ULOF transient have been described in details thanks to generic event trees (GETs) and phenomenological event charts (PECs) in the second part of the paper. This has been done in the frame of a Japanese/French collaboration (involving JAEA, MFBR, Framatome and CEA). GETs describe the whole event to identify possible range of event sequences according to physics. It enables to draw a fruitful common understanding of the event evolution and to structure the PIRT exercise presented at the end of the paper. The same PIRT exercise will be carried-out for UTOP and USAF by taking benefit of this first ULOF PIRT exercise.

Acknowledgment

The authors would like to thank the Nuclear Support and Innovation Division of CEA which has supported and contributed to this work as well as the SFR R&D and SFRAG project managers.

Present study includes the result of "Technical development program on a fast reactor international cooperation, etc." entrusted to JAEA by the Ministry of Economy, Trade and Industry (METI).

References

Bachrata A. et al., Code Simulation of Quenching of a High Temperature Debris Bed: Model Improvement and Validation With Experimental Results, ICONE20-POWER2012-54221, Anaheim (USA), August 2012.

Bachrata A. et al., 2015. Unprotected Loss of Flow simulation on ASTRID CFV-V3 reactor core, Proceedings of ICAPP 2015, May 03-06, 2015 - Nice (France), Paper 15356

Bertrand F. et al., 2016. Comparison of the behaviour of two core designs for ASTRID in case of severe accidents. Nuclear Engineering and Design. 297, 327–342

Bachrata A. et al., 2019. A three-dimensional neutronics – Thermalhydraulics Unprotected Loss of Flow simulation in Sodium-cooled Fast Reactor with mitigation devices, Nuclear Engineering and Design, 346, pp. 1-9, 2019.

Bertrand F. at al., 2018. Status of severe accident studies at the end of the conceptual design of ASTRID: Feedback on mitigation features. Nuclear Engineering and Design 326 (2018) 55–64

Chellapandi, P. et al., 2013. Primary containment capacity of prototypefast breeder reactor against core disruptive accident loadings. Nuclear Engineering and Design 256.

Droin J.B., 2016. Modélisation d'un transitoire de perte de debit primaire non protégé dans un RNR_Na. Thèse de Doctorat, Université Grenoble-Alpes, 2016.

Droin J.B. et al., 2017. Physical tool for Unprotected Loss Of Flow transient simulations in a Sodium Fast Reactor, Annals of Nuclear Energy, 106, pp. 195-210.

European expert network for the reduction of uncertainties in severe accident safety issues (EURSAFE), NED 235 (2005) 309-346

Gauthé P. and Sciora P., 2017. Sensitivity studies of SFR unprotected transients with global neutronic feedback coefficient. International Conference on Fast Reactors and Related Fuel Cycles, FR17, Yekaterinburg, Russia, June 26-29, 2017.

Geffraye G. et al., 2011. CATHARE 2 V2.5_2: A single version for various applications, Nuclear Engineering and Design, Vol. 241, Issue 11

GIF, 2002. A technology roadmap for Generation IV Nuclear Energy Systems, US DOE and the Generation IV International Forum

Herbreteau K. et al., 2018. Sodium-cooled fast reactor pin model for predicting pin failure during a power excursion, Nuclear Engineering and Design, 335, 279-290

Kubo, S., Shimakawa, Y., 2015. JSFR design progress related to development of safety design criteria for generation IV sodium-cooled fast reactors (2). Progress of safety design. In:23rd International Conference on Nuclear Engineering, Paper 1748, 2015, Chiba, Japan.

Le Coz P. et al., 2013. The ASTRID Project: status and future prospects, proceedings of FR13, Paris France 4-7 March 2013. Paper CN 199-261

Lemasson D. and Bertrand F., 2014. Simulation with SAS-SFR of a ULOF transient on ASTRID-like core and analysis of molten clad relocation dynamics in heterogeneous subassemblies with SAS-SFR, ICAPP 2014, Charlotte, NC, April 6-9, 2014, pp. 558-567

Manchon, X. et al., 2017. Modeling and Analysis of Molten Fuel Vaporization and Expansion for a Sodium Fast Reactor Severe Accident, Nuclear Engineering and Design, November 2017, 322, pp. 522-535.

Marie N. et al., 2016a. Physico-statistical approach to assess the core damage variability due to a total instantaneous blockage of SFR fuel sub-Assembly, Nuclear Engineering and Design, Volume 297, February 2016, Pages 343-353

Marie N. et al., 2016b. A physical tool for severe accident mitigation, Nuclear Engineering and Design, Volume 309, 1 December 2016, Pages 224-235

Maschek W., et al., Prevention and mitigation of severe accident developments and recriticalities in advanced fast reactor systems, Progress in Nuclear Energy 53 (2011), 835-841

Maschek W., et al., Investigation on upper bounds of recriticality energetics of hypothetical core disruptive accidents in sodium cooled fast reactors, Nuclear Engineering and Design, 326 (2018), 392-402

PIRT: R&D priorities for loss-of-cooling and loss-of-coolant accidents in Spent Nuclear Fuel Pools, OECD/NEA Report of 2018

Ruggieri, J.M., et al., 2006. ERANOS 2.1: International Code System for GEN IV Fast Reactor. ICAPP 2006, Reno, USA.

Sciora P. et al., 2011. Low void effect core design applied on 2400 MWth SFR reactor, proceedings of ICAPP 2011, Nice, France

Serre F. et al., France-Japan collaboration on the severe accident studies for ASTRID: Outcomes and future work program, Proceedings of 2017 International Congress on Advances in Nuclear Power Plants, ICAPP 2017 - A New Paradigm in Nuclear Power Safety.

Sridi M. et al., 2016. Cache Aware Dynamics Data Layout for Efficient Shared Memory Parallelisation of EUROPLEXUS, Procedia Computer Science, Volume 80, 2016, Pages 1083–1092

Suzuki T. et al., A scenario of core disruptive accident for Japan sodium-cooled fast reactor to achieve in-vessel retention, Journal of Nuclear Science and Technology, 2014, Vol. 51, No. 4, 493–513

Waltar, A.E., Reynolds, A.B., 1981. Fast Breeder Reactors. Pergamon Press Inc., New York

Yamano, H. et al., 2003. SIMMER-IV: A Three-dimensional Computer Program for LMFR core Disruptive Accident Analysis, Version 2. A Model Summary and Program Description, JNC Report. Japan Atomic Energy Agency, JNC TN9400 2003-070.